EUROPEAN ORGANIZATION FOR NUCLEAR RESEARCH

CERN-EP/89-164
December 15th, 1989

The beta decay of ^{9}Li to levels in ^{9}Be: a new look

G. Nyman[1], R.E. Azuma[2], P.G. Hansen[3], B. Jonson[1], P.O. Larsson[1], S. Mattsson[1], A. Richter[4], K. Riisager[5], O. Tengblad[1], K. Wilhelmsen[1], and The ISOLDE Collaboration[5]

(IS01-3)

Keywords

RADIOACTIVITY ^{9}Li(β^-) [from UC+p reaction]; measured β-delayed neutrons and alpha particles. Deduced branching ratios and reduced transition probabilities. R-matrix analysis. Surface barrier Si detectors, ^{3}He spectrometers, on-line mass separation.

Abstract

Beta-delayed neutrons and alpha particles from the decay of ^{9}Li have been studied with a ^{3}He neutron spectrometer and silicon surface barrier detectors. The data show that the 50 ± 3 % feeding to particle unbound states mainly proceeds to the four excited states in ^{9}Be at 2.43 MeV (30 ± 3 %), 2.78 MeV (16 ± 3 %) and 11.28 MeV + 11.81 MeV (3.8 ± 0.2%). The strong feeding to the 11.81 MeV state observed corresponds to a log ft value of 2.84. The beta decay rates are strongly affected by the broad levels populated in the decay. Corrections involving R-matrix calculations have been applied for the extraction of the reduced transition probabilities. We confirm the recently determined strong asymmetry in the beta decays of the 3/2$^-$ ground states of ^{9}C and ^{9}Li to the excited 5/2$^-$ states in the daughters ^{9}B and ^{9}Be.

---

[1] Dept. of Physics, Chalmers University of Technology, Göteborg, Sweden
[2] Dept. of Physics, Univ. of Toronto, Ontario, Canada
[3] Inst. of Physics, University of Aarhus, Aarhus, Denmark
[4] Institut für Kernphysik, Technische Hochschule, Darmstadt, Fed.Rep. of Germany. Supported by the Bundesministerium für Forschung und Technologie of the Federal Republic of Germany under the contract number 06DA454
[5] CERN, Geneva, Switzerland

Accepted for publication in Nucl. Phys. A.

1. Introduction.

Experimental studies of extremely neutron-rich nuclei remain a major challenge in the current research on nuclei far from stability. In spite of a painstaking effort over many years to develop new methods to produce neutron-rich nuclei, most of the predicted particle-stable species remain experimentally inaccessible. It is only for the lightest elements that, during the last years, the limit of prompt neutron instability – the neutron drip-line – has been reached. A review of recent progress is given in ref. [1].

The theoretical understanding of neutron-rich nuclei has until now been based on simple extrapolations of models that work for the well-studied nuclei close to beta-stability, but new experimental data indicate that novel features appear at the neutron drip-line. The first indication came from a measurement by Tanihata and co-workers [2] of matter radii of lithium isotopes. The radius stays roughly constant for the isotopes with mass numbers from $A = 6$ to $A = 9$ but increases drastically for ^{11}Li (the isotope ^{10}Li is unbound to neutron emission). It is possible to explain [3] the large matter radius of ^{11}Li from the fact that the last pair of neutrons in ^{11}Li has very low binding energy ($B_n = 250 \pm 80$ keV) and therefore forms a neutron halo around the ^{9}Li core.

This work deals with the decay of the lithium isotope ^{9}Li, also a drip-line nucleus. (It is the most neutron-rich of the $A = 9$ isobars. We have deduced its beta-strength function from studies of delayed neutron and delayed alpha data. As all excited states in the daughter, ^{9}Be, break up into two alpha particles and one neutron the complete decay scheme can be constructed from these data. The study is complicated both by the large widths of the levels fed in ^{9}Be through the beta decay and by the subsequent break-up that often takes place via broad intermediate states. These effects make the spectra almost featureless. A complete outline of our procedure to treat these complications is given in appendix A.

1.1 Previous work

The first experimental identification of ^{9}Li as a beta-delayed neutron emitter was made by Gardner et al. [4] in 1951. The lithium activity in this experiment was produced in a ^{9}Be(d,2p)^{9}Li reaction and the half-life was determined to be 168 ms. The mass excess of ^{9}Li was determined [5] from a ^{7}Li(t,p)^{9}Li reaction where the Q-value of -2.386 MeV gives a mass excess of 24.9537 MeV. This together with the ^{9}Be mass excess [6] gives a Q_β = 13.606 MeV.

Alburger [7] measured the energy spectrum of beta particles from ^{9}Li and observed two components with endpoints of 13.5 $\pm$ 0.5 MeV and 11.0 $\pm$ 0.4 MeV, respectively, the latter component resulting from a measurement performed in coincidence with neutrons. From this experiment he deduced a 25 % feeding to the ^{9}Be ground state. The remaining intensity was suggested to be due to feeding of an excited state at 2.43 MeV. The beta-coincident neutron spectrum was recorded in a plastic scintillator and the main component showed neutrons with an energy of around 0.7 MeV. There was also evidence for neutrons of higher energy. Alburger and Wilkinson [8] produced ^{9}Li in an ^{3}H(^{7}Li,p)^{9}Li reaction and measured its half-life with high precision. Their value of 178.3 $\pm$ 0.3 ms has been adopted as the best value for the ^{9}Li half-life.

Measurements of the energy spectra of delayed neutrons from ^{9}Li were performed by Chen et al. [9] and by Macefield et al. [10]. In both these studies the neutron spectra were measured with a time-of-flight technique, but substantial differences in the beta branching ratios were obtained. Chen et al. found that 65 $\pm$ 3 % of the beta-decay feeds the ^{9}Be ground state and that the remaning 35 % of the decay feeds neutron-unbound excited states. This latter number was for several years taken to be the P_n value for ^{9}Li and several determinations of delayed-neutron branching ratios for other precursors were given relative to this value.

In a new determination of the ^{9}Li neutron branching ratio in 1981 Bjørnstad et al. [11] used a technique by which beta-neutron coincidences were recorded. The beta particles were counted with a 1 mm thick plastic scintillator and the neutrons in a 4π paraffin moderated neutron counter. The beta-neutron time distribution was recorded together with the singles rates. The P_n value was obtained

from the ratio between singles beta-particles and βn coincidences corrected for the neutron detection efficiency. A careful calibration of the neutron detector then gave the delayed neutron branching ratio for ^{9}Li as 50 $\pm$ 4 %. This new value of the branching ratio was confirmed in an experiment by Langevin et al [12] who deduced the P_n value from a study of the beta-delayed alpha-spectrum. From these two determinations we adopt the value P_n = 50 $\pm$ 3 %.

The data presented in this paper allow a determination of the absolute beta feedings to the excited states in ^{9}Be. In line with the findings of Langevin et al. [12] we find evidence for a strong feeding to the highly excited states in ^{9}Be. The fairly large mirror-decay asymmetry [13] between the ^{9}C and ^{9}Li decays to the excited 5/2$^-$ states in ^{9}B and ^{9}Be, respectively, has been confirmed.

2. Experimental procedures.

The ^{9}Li radioactivity was produced by bombarding a 13 g/cm^2 uranium carbide target kept at 2000 ^{0}C with a beam of 1.6 μA protons from the CERN Synchrocyclotron. The lithium atoms were ionized in a W-surface ionization source [14] and subsequently mass separated in the ISOLDE on-line mass separator. The ^{9}Li$^+$ beam of typically 3×10^6 atoms/sec was directed to the experimental set-up by means of an external beam line. The experiment was performed in a room one floor above the isotope separator in order to reduce the neutron background from the ISOLDE target.

Fig. 1 shows the decay scheme of ^{9}Li. Given a Q_β value of 13.606 MeV and with 50 % of the feeding to states above the neutron separation energy, the study of the delayed neutron spectrum is important for a determination of the feeding to excited states. As seen in the figure all levels in ^{9}Be above the three-body break-up threshold can, apart from the n + ^{8}Be channel, decay also through ^{5}He + α due to the width of the ^{5}He ground-state. Since the ^{5}He and ^{8}Be nuclei subsequently break up into n + α and α + α, respectively, a complete study must also contain a measurement of the delayed alpha spectrum. The energies and widths of the states were taken from the compilation of Ajzenberg-Selove [15] and are given in table 1.

The delayed-neutron spectra from the ^{9}Li decay were measured with a gridded ^{3}He-filled proportional counter placed in a shielding box consisting of layers of paraffin, polyethylene and cadmium. The distance from the ^{3}He spectrometer to the walls of the shielding was 1.5 m at minimum in order to minimize detection of scattered ^{9}Li delayed neutrons from the walls. The background inside the shielding box was less than 0.01 neutrons/min as measured by the proportional counter. The shielding also acted as a protection against acoustic noise pick-up on the long central wire of the proportional counter. The FWHM energy resolution of the detector, at optimal conditions, is 12 keV at thermal energies and increases smoothly to about 20 keV at 1 MeV neutron energy. To get the intensity distribution a correction for the energy dependent detector efficiency was performed. The main features of the detector efficiency were given by Franz et al. [16] up to an energy of about 3 MeV; the response at low energies follows the 1/v law of the ^{3}He(n,p)^{3}H reaction but drops sharply above 1 MeV. A recent, more careful, study of the detector response [17] has revealed a number of new features, especially at low energies. The response is complex due to the distribution of the recoiling hydrogen and helium nuclei and to resonance scattering in the steel wall of the spectrometer.

A special study of the shape of the 682 keV peak in the neutron spectrum was carried out with a time-of-flight experiment in which the time interval between the beta particle and a neutron was registered. The beta particles were detected using a 1 mm thick Pilot U plastic scintillator and the neutrons by two 1/2″(thickness)×5″(diameter) NE110 plastic scintillators. The flight paths for the neutrons were 103 cm and 52 cm, respectively. The two neutron detectors were placed at different angles with respect to the beta detector. Thus the recoil effects on the 682 keV peak could be studied as a function of the beta-neutron angle.

For the alpha spectroscopic measurements the ^{9}Li ion beam was stopped in a 40 μg/cm^{2} carbon foil placed in front of a thick silicon surface barrier detector with an energy resolution of 25 keV FWHM at 5 MeV alpha energy.

3. Experimental results.

The energy spectrum of beta-delayed neutrons from ^{9}Li is shown in fig. 2. The spectrum has been corrected for the energy dependence of the detector efficiency. The main features of the shape agree with the time-of-flight spectra obtained by Chen et al. [9] and Macfield et al. [10]. The thermal peak, mainly due to ^{9}Li neutrons thermalized inside the shielding box, has been subtracted from the spectrum in fig. 2. The spectrum shows broad neutron distributions above and below the relatively narrow 682 keV peak. The intensity below the 682 keV peak (fig. 5) has a structure in the energy region up to about 250 keV. This structure was shown by Tengblad et al. [18] to be due to neutron scattering in the steel wall of the ^{3}He spectrometer and can completely be accounted for by known resonances in ^{56}Fe.

Part of the structure of the broad bump below the 682 keV peak could be due to the neutron emission from the $1/2^{+}$ level at 1.68 MeV in ^{9}Be to the ground state of ^{8}Be. The contribution from this level, however, cannot be seen directly in the neutron spectrum (fig. 2) due to the much more intense neutron emission from higher excited states in ^{8}Be. The pronounced asymmetric shape of the $1/2^{+}$ level is displayed in fig. 3 by the sum (to enhance the statistics) of three recently measured inelastic electron scattering spectra of ^{9}Be. One of the prime motivations for this ^{9}Be(e,e') experiment was to verify the peculiar (but now explained [18]) fine structure at low energies in the neutron spectrum. The ^{9}Be(p,p') spectra are also structureless [19].

Fig. 4 shows the delayed alpha spectum from ^{9}Li. Two structures can be observed, a bump at low energy and a high energy tail. The latter distribution stems from decays via the excited states around 11.5 MeV in ^{9}Be.

The low-energy part of the beta-delayed neutron spectrum is shown in fig. 5. In the inset the 682 keV peak (see section 4.1) is shown after subtraction of neutrons originating from other decay channels and compared to the calculated shape. In the calculation effects of recoil broadening and polarization (see appendix B) are included.

4. Decay scheme.

4.1 The beta decay to levels in ^{9}Be

In order to extract information on the beta-feeding to excited states in ^{9}Be one has to take into account that the daughter states, after both beta decay and particle emission, in most cases are broad. Also recoil effects have to be taken into account and this gives rise to a relatively complicated procedure to extract the absolute beta feeding. The main ideas in our treatment of the data are given in ref. [20] and in the appendices. Note that only sequential decay of the states in ^{9}Be is included.

The neutron separation energy in ^{9}Be is 1.6654 MeV and all excited states are thus unstable to neutron break-up. The spin and parity of the first excited state at 1.68 MeV have been determined to be $1/2^+$ [15]. The excitation energy and width were recently measured very precisely [19] from ^{9}Be(e,e') and ^{9}Be(p,p') reactions to be 1.684 ± 0.007 MeV and 217 ± 10 keV, respectively. If this state is fed in the beta decay its deexcitation may proceed either by γ emission or by neutron emission. Due to its width a weak neutron branch from it would be obscured in the neutron spectrum (fig. 2) by contributions from higher excited states. An analysis of our data allows an upper limit of 2 % feeding to this level.

The states from 2.43 MeV and up to the top of the excitation spectrum are all assumed to decay entirely by particle emission and from the P_n value one gets a total beta intensity of 50 ± 3 % to these states. The possible decay channels are:

a) $^9\mathrm{Be}^* \rightarrow {}^8\mathrm{Be}(0^+) + \mathrm{n}$, $^8\mathrm{Be} \rightarrow \alpha + \alpha$

b) $^9\mathrm{Be}^* \rightarrow {}^8\mathrm{Be}(2^+) + \mathrm{n}$, $^8\mathrm{Be} \rightarrow \alpha + \alpha$

c) $^9\mathrm{Be}^* \rightarrow {}^5\mathrm{He}(3/2^-) + \alpha$, $^5\mathrm{He} \rightarrow \mathrm{n} + \alpha$

d) $^9\mathrm{Be}^* \rightarrow {}^5\mathrm{He}(1/2^-) + \alpha$, $^5\mathrm{He} \rightarrow \mathrm{n} + \alpha$

The 682 keV peak in the spectrum is due to the neutron decay from the $5/2^-$ state at 2.43 MeV in ^{9}Be to the ground state of ^{8}Be. The width (0.77 keV) of the 2.43 MeV state corresponds to a lifetime of 8.5×10^{-19} s. This short lifetime implies that the delayed neutron is emitted before the

beta-recoiling ^{9}Be nucleus has come to rest and the peak will thus be recoil-broadened. The spectrum in fig. 5 clearly displays this recoil effect where the measured peak is considerably broader than the instrumental resolution at 682 keV. The inset also shows the calculated peak shape obtained when, besides the detector resolution, also the beta-recoil energy distribution and anisotropy effects are included. The calculation follows the outline given in refs [20,21] but for completeness the main formulas are given in appendix B.

The excited 2^+ state in ^{8}Be at 2.94 MeV has a width of 1.56 MeV and a large fraction of the neutron decay from the 2.43 MeV state proceeds to the tail of this state. The broad distribution of neutrons up to the 682 keV peak is partly due to this feeding. A large contribution also comes from the decay channel **c**. The relative intensities of these two contributions to what we will call the 300 keV bump are roughly 2:1.

The 300 keV bump and the 682 keV line are superimposed on a continuum of neutrons originating from higher excited states in ^{9}Be. This intensity stems mainly from neutron emission of the $1/2^-$ state at 2.78 MeV in ^{9}Be. The decay of this state proceeds through channels **a**, **b** and **c**. The low energy part of the neutron spectrum is thus built up from decay of the 2.43 MeV state, which is responsible for the bump and the peak, and the 2.78 MeV state which accounts for most of the broad distribution beneath. The contributions from levels with higher excitation energies are essentially constant or slightly decreasing towards the low energy end of the spectrum. Their contribution at energies above 3 MeV cannot be seen in the spectra recorded by the ^{3}He spectrometer due to the strong drop in the detector efficiency above this energy. From the fit we can extract the absolute intensity of beta feeding to these two states to be 30 $\pm$ 3 % and 16 $\pm$ 3 %, respectively.

The high energy part of the neutron spectrum is due to feeding of excited states above the 2.78 MeV state. The best possibility to obtain the beta feeding to states at high excitation energies is, however, offered by the high-energy part of the delayed alpha spectrum shown in fig. 4. We start with the two states at 11.28 MeV and 11.81 MeV. These states decay mainly via channels **b**, **c** and **d**, where the high energy alpha particles originate from the decay through ^{5}He. A fit of the high energy part of the

alpha spectrum, shown in fig. 4, gives a clear indication that the main part of the feeding proceeds via the 11.81 MeV state. This is in contradiction with the finding by Langevin et al. [12] who exclude any feeding to the 11.81 MeV state. The explanation for this difference in interpretation comes from the assumption made by Langevin et al. that the intermediate state in ^{9}Be directly breaks up into two alpha particles and a neutron. This gives larger phase space for decays with high alpha-particle energy and the observed maximum energy can thus be explained as due to the 11.28 MeV state only. The steep fall-off at the endpoint of the singles spectrum is, however, difficult to explain with a direct three-body break-up; the phase space alone would give a smoother endpoint region of lower intensity and incorporation of final state Coulomb and strong interactions would give a further decrease of the intensity there (as the endpoint corresponds to decays with two low-energy particles). The very accurate fit to the endpoint of the alpha spectrum (see inset of fig. 4) favours the interpretation that the main part of the beta-feeding to high excitation energies in the daughter nucleus goes to the 11.81 MeV state. A good fit can be obtained with this state alone, but by allowing up to 30 % of the intensity in this region to be due to the 11.28 MeV state an improvement of the fit is achieved.

In order to get the total beta intensity to highly excited states one has to combine the results of the analysis of the delayed neutron and the delayed alpha spectra. At energies below 1 MeV the singles alpha spectrum shows a tail due to beta pile up. The best fit to the experimental data at high energies (inset of fig. 4) gives 3.8 $\pm$ 0.2 % as the absolute beta-feeding to the 11.81 MeV and 11.28 MeV states. Including beta-feeding to the excited states at 2.43 MeV, 2.78 MeV,11.28 MeV and 11.81 MeV gives the fit to the delayed neutron spectrum as illustrated by the full drawn curve in fig. 2. The data give no clear evidence for feeding of the 7.94 MeV state; an upper limit of 2 % can be given for decay through channels **b**, **c** and **d** (these channels give high energy alphas, the limit for channel **a** is only 5 % as it gives high energy neutrons and low energy alphas – both hard to detect). The limit of 2 % is consistent with the 1.5 $\pm$ 0.5 % of ref. [12].

Column 4 of table 2 summarizes our results. Interference between levels is not included here but could occur. This would change the spectral shapes away from the resonances and thus the

beta-feedings, but is not expected to change the extracted B(GT)-values substantially: As an example the intensity from the 11.81 MeV level, shown as a fit in the inset of fig. 4, would change in the energy region below 3 MeV. On the other hand the correction factor R' (to be discussed below) changes correspondingly so that the extracted B(GT)-value to a good approximation will be unaffected.

4.2 The particle emission from levels in ^{9}Be.

The data are not complete enough to determine the break-up mechanism of the excited states in ^{9}Be unequivocally. The fit in ref. [12] included direct three-body break-up and sequential decays through states in ^{8}Be, but not through states in ^{5}He. We have found that the beta-delayed spectra can be fitted with sequential decays, only, when the decays through ^{5}He are included. The break-up to "two alphas + one neutron" of ^{9}Be could be expected to be similar to the break-up to "one alpha + two nucleons" of the mass 6 nuclei. Here a recent detailed study [22] of the 2^+ states showed the sequential decays to be dominating.

The analysis emphasizes the extraction of the beta-feeding so that only rough branching ratios for the particle decay channels of the excited states in ^{9}Be can be extracted. These could in any case not be compared directly to particle branching ratios found in nuclear reactions as explained in the next section.

5. Discussion.

We have, in this work, determined the beta feedings from ^{9}Li to states in ^{9}Be. Besides the ground state feeding of 50 % determined from the P_n value [11,12] there is strong beta feeding to four excited states. This general pattern is in agreement with the decay [13] of the mirror nucleus ^{9}C. For the beta decay to the ground state ($3/2^-$) and the narrow 2.43 MeV state (Γ = 0.77 keV, $5/2^-$) the log ft values and the reduced transition probabilities, B(GT)$^-$, can be determined using standard methods. For the broad states at 2.78 MeV, 11.28 MeV and 11.81 MeV it is not trivial and it will be shown that there is a considerable difference in the values obtained from a complete analysis, as outlined in appendix A, and an analysis without any adjustment for the widths of the states involved.

With the adopted value of 50 ± 3 % for the ^{9}Li P_n value we get log ft = 5.32 for the $3/2^- \rightarrow 3/2^-$ ground-state to ground-state transition. The prescription given in ref. [23] is used for the calculation of the statistical rate function. The corresponding Gamow-Teller reduced transition probability is obtained from equation (1) in appendix A. This gives $B(GT)^- = 0.019 \pm 0.002$. The δ factor used by Wilkinson in his works [24,25] and defined as:

$$\delta = \frac{(ft)^+}{(ft)^-} - 1$$

then becomes $\delta = -0.09 \pm 0.16$.

For the feeding to the 2.43 MeV state in ^{9}Be we get log ft = 5.13 and $\delta = 1.2 \pm 0.5$. The large uncertainty in the δ-value is mainly due to the 35 % uncertainty in the feeding to the 2.36 MeV mirror state in ^{9}B. Mikolas et al. [13] used an alternative asymmetry parameter defined as:

$$\Delta = \sqrt{B(GT)^-} - \sqrt{B(GT)^+}$$

which for the present measurement gives $\Delta = 0.06 \pm 0.03$. (Note that we, in our calculations, have neglected quenching of the axial vector coupling constant and that the value for Δ given in ref. [13] is based on a definition of B(GT) which differs from the one given in appendix A.) This is larger than the prediction of $\Delta = 0.008$ by Towner [26], who calculated the deviations from mirror symmetry in the systems; these differences are mostly due to the different binding energies and thus stem from the difference in the Coulomb-interaction. Our new data thus do not confirm the suggestion by Mikolas et al. [13] of a systematic misinterpretation of the ^{9}Li data in earlier work.

The broad states at 2.78 MeV, 11.28 MeV and 11.81 MeV are treated with the procedure of appendix A. The correction factors R′ are 2.7, 1.5 and 1.9 with uncertainties around 20% for the 2.78 MeV, 11.28 MeV and 11.81 MeV states, respectively, giving the B(GT) values in table 2. As should be clear from the discussion in the appendix this procedure is dependent on the assumed decay mechanism. The total correction factor for a level depends on the branching ratios of the different particle emission channels and the extracted B(GT) values are therefore necessarily more uncertain than the beta-feedings. The particle branching ratios will of course also be affected by the skew beta-feeding of the levels, making a direct comparison with reaction data impossible.

The B(GT)$^-$ value for the 2.78 MeV state, which naively would be 0.018 $\pm$ 0.003, then becomes 0.007 $\pm$ 0.003. Similarly, the B(GT)$^-$ value for the 11.81 MeV state drops to about 5.6. The "naive" value that exceeds 10 would be hard to reconcile with the sum-rule Σ B(GT)$^-$ $-$ Σ B(GT)$^+$ = 3(N$-$Z) = 9; this only accentuates the need for a proper treatment of the broad levels. As already mentioned we only have an upper limit on the beta-feeding to the 7.94 MeV level. Here the correction factors turn out to be less than one (i.e. the level is positioned favourably with both a large f-factor and large particle penetrabilities – broadening the level only decreases the product of these and thereby decreases the total decay probability) so that our corrected limit on the B(GT)$^-$ to this level is 0.25.

To make a meaningful comparison with the data from ^{9}C the corresponding correction must of course be made for the broad levels in ^{9}B. Unfortunately, the branching ratios for particle decay are not known here; we can therefore only make an estimate of the correction based on the theoretical branching ratios given in ref. [13]. We get an upper limit on B(GT) for both the 5/2$^-$ level at 2.361 MeV and the 1/2$^-$ level at 2.79 MeV, but no reliable lower limit. In the first case the limit is 0.009 $\pm$ 0.003, in the second case 0.012 $\pm$0.005. The correction therefore again enlarges the difference between the 5/2$^-$ levels in ^{9}Be and ^{9}B, whereas there is agreement within the rather large errors for the 1/2$^-$ levels.

6. Conclusion

As all excited states in ^{9}Be are unstable with respect to break-up into (ultimately) two alpha particles and a neutron, the decay of ^{9}Li is rather complex. Effects of the beta-recoil or of the broad states in the decay chain are here shown to be of importance for the interpretation of a major part of the decays. Our approach of treating the decays to broad levels is, although not perfect, capable of giving first order corrections to the beta feedings, so that the matrix elements for the beta decay can be extracted. In particular for the decay to the 11.81 MeV level, the standard procedure for calculating an ft value using the Q value, the excitation energy and branching ratio would be highly misleading.

The data were compared with data [13] on the corresponding mirror decay of ^{9}C. The existing indications of a large mirror asymmetry between the two systems are confirmed.

No detailed comparison with theory has been made. Mikolas et al. [13] have carried out shell-model calculations for the mass 9 nuclei and give B(GT) values for four different interactions. Unfortunately, the results for the different interactions scatter too much to allow quantitative comparisons with the data. The main trends are, however, reproduced.

Acknowledgments We are grateful to M.J.G. Borge, T.E.O. Ericson, K.-L. Kratz and W. Ziegert for discussions and help.

Appendix A

Beta decay involving broad levels.

A standard problem when modelling a physical system is the delimitation of the system, be it in space or in time. The problem appears also for beta decays to unstable levels: this is a multistep process and it is not a priori clear in which cases the beta decay and the decay of the unstable level can be treated separately. One would expect narrow levels to behave approximately like stable states, i.e., one can disregard that they are unstable, whereas broad levels could behave differently. The levels that enter in the decay of mass 9 nuclei are clearly broad and must be considered with care. The distinction between narrow and broad levels is, however, not obvious in the general case; to give an example, it turns out [27] that the appropriate energy scale in the related process, electron capture (where the relevant excited states after the weak decay are atomic and not nuclear), is the one of the atomic radiation, i.e., a few keV, and not the typical one MeV of the weak decay. A quantitative criterion for when a level is broad can only be given if a theory involving the broad levels exists; this appendix purports to collect the existing formalism relevant for beta decays. The expressions used in our fits to the data are given in eqs. (5) and (10) and the R-factors, used for correcting the B(GT)-values for effects of the broad levels, are given in eqs. (8) and (11).

In standard presentations of beta decays only stable final states are discussed. The decay rate is given by the product of a matrix element squared and a phase space factor. The ft-value for allowed decays is defined by

$$ft = \frac{K}{G_V^2 B(F) + G_A^2 B(GT)} , \qquad (1)$$

where B(F) and B(GT) are the Fermi and Gamow-Teller reduced transition probabilities with the constants [28,29] $K/G_V^2 = 6141 \pm 4$ s and $(G_A/G_V)^2 = 1.59 \pm 0.01$. The ft-value can here be thought of as a comparative half-life (partial half-life corrected for the phase space factor) or, alternatively, as a measure of the matrix element for the transition. The first interpretation is difficult to extend to broad levels due to the variation of the f-factor across a level; we must therefore work in terms of the matrix

elements directly and only use the formula above at the end, if a log ft value for the transition to the broad level is wanted.

As a starting point we shall here use the R-matrix theory as applied to beta decays by Barker and Warburton [30,31,32,33]. For the case – sketched in fig. 6a – of a daughter nucleus with many levels λ and only one decay-channel open they give the beta decay probability, $w(E)$, per unit energy interval with E being the excitation energy in the daughter nucleus:

$$w(E) = f_\beta(Q-E)\sum_l P_l(E-E_f)\frac{\left|\sum_\lambda\{g_\lambda^F\gamma_{\lambda l}/(E_{\lambda l}-E)\}\right|^2 + \left|\sum_\lambda\{g_\lambda^{GT}\gamma_{\lambda l}/(E_{\lambda l}-E)\}\right|^2}{\left|1-\{S_l(E-E_f)-B_l+iP_l(E-E_f)\}\sum_\lambda\{\gamma_{\lambda l}^2/(E_{\lambda l}-E)\}\right|^2}\ , \qquad (2)$$

where P_l and S_l are the usual penetration and shift factors (P_l includes the phase space factor for the emitted particle), $E-E_f$ the c.m. energy of the emitted particle, B_l a boundary parameter to be chosen at will, $E_{\lambda l}$ the position parameter of the level (not necessarily equal to the resonance energy), γ the reduced width, g the corresponding width for beta-decay, f_β the statistical rate function and l the angular momentum. A normalization constant C introduced in ref. [30] can be included in the factor g and is therefore omitted here, for other treatments see refs [30,33] (who implicitly assume this normalization factor to be the same for broad as for narrow levels, thus removing it via the normalization to narrow levels). The relation between the widths g and the reduced transition probabilities B(F) and B(GT) employed in (1) is most conviently found by taking the limit of narrow levels [30,33]. For a single level λ one takes $B_l = S_l(E_\lambda - E_f)$, use that in the limit $\Gamma_\lambda = 2\gamma_\lambda^2 P_l(E_\lambda - E_f)$ and integrate over the resonance to get:

$$w = f_\beta(Q-E_\lambda)\pi\{(g_\lambda^F)^2 + (g_\lambda^{GT})^2\}\ . \qquad (3)$$

By comparing (1) and (3) one gets

$$(g_\lambda^F)^2 = \frac{\ln 2}{\pi K}G_V^2 B(F) \qquad \text{and} \qquad (g_\lambda^{GT})^2 = \frac{\ln 2}{\pi K}G_A^2 B(GT)$$

and thus the general formula:

$$w(E) = \frac{\ln 2}{\pi K} f_\beta(Q-E) \sum_l P_l(E-E_f) \frac{\left|\sum_\lambda \{G_V M_\lambda^F \gamma_{\lambda l}/(E_{\lambda l}-E)\}\right|^2 + \left|\sum_\lambda \{G_A M_\lambda^{GT} \gamma_{\lambda l}/(E_{\lambda l}-E)\}\right|^2}{\left|1-\{S_l(E-E_f)-B_l+iP_l(E-E_f)\}\sum_\lambda \{\gamma_{\lambda l}^2/(E_{\lambda l}-E)\}\right|^2} , \quad (4)$$

where $(M_\lambda^i)^2 = B(i)$, i = F,GT.

The structure of the formula is understood better in the simpler case of one single intermediate level with no Fermi-feeding, i.e. B(F) = 0. Equation (4) then reduces to:

$$w(E) = \frac{\ln 2}{\pi K} f_\beta(Q-E) \sum_l \frac{G_A^2 B(GT)\, P_l(E-E_f)\gamma_{\lambda l}^2}{(E_{\lambda l}+\Delta_{\lambda l}(E)-E)^2 + (\frac{1}{2}\Gamma_{\lambda l}(E))^2} , \quad (5)$$

$$\Delta_{\lambda l}(E) = -(S_l(E-E_f)-B_l)\gamma_{\lambda l}^2 , \quad \Gamma_{\lambda l}(E) = 2P_l(E-E_f)\gamma_{\lambda l}^2 .$$

This resembles a standard Breit-Wigner shape, but contains in the numerator the energy variation of the f-factor and the penetration factor and in the denominator a contribution from the shift and penetration factors (note that the penetration factor in the numerator disappears by integration over a narrow level; the intensity is therefore not affected linearly by the penetration factor as eq. (5) could lead one to think, but only through the change of shape it brings about). A level is therefore "narrow" – in the sense that eq. (1) can be used – when the variation of f(Q−E), $P(E-E_f)$ and $S(E-E_f)$ across the level is small. With the approximation $f(Q-E) \approx (Q-E)^5$ and demanding $|\frac{\partial f}{\partial E}\Gamma| \ll f$, where Γ is the full width at half maximum of the level, one sees that levels must fulfil

$$5\Gamma \ll Q-E \quad (6)$$

to be called narrow. Similarly, the requirement $|\frac{\partial P}{\partial E}\Gamma| \ll P$ leads for s-wave neutrons to

$$\Gamma \ll E-E_f \quad . \quad (7)$$

The penetration factors for charged particles and for higher angular momenta give rise to more complex expressions and will not be given here.

The above criteria for "narrowness" are useful for a rough distinction, only. We obtain a quantitative measure by taking the ratio of the integrated decay probability $w = \int w(E)dE$, with $w(E)$ from eq.

(5), to the decay probability w_0 for a narrow level given in eq. (3). This ratio, R, becomes

$$R = \frac{1}{\pi}\int_{E_f}^{Q} dE\,\frac{f_\beta(Q-E)}{f_\beta(Q-E_\lambda)}\sum_l \frac{P_l(E-E_f)\,\gamma_{\lambda l}^2}{\left|(E_\lambda - E) - \{S_l(E-E_f) - B_l + iP_l(E-E_f)\}\gamma_{\lambda l}^2\right|^2} \quad . \tag{8}$$

The ratio differs from Barker's [30,31] quantity I_λ in including the f-functions explicitly and in being normalized to unity for a narrow level. It can be interpreted as the change in intensity due to the broadness of the level. The intensity can decrease as well as increase, as seen e.g. in the emission of $\ell = 1$ neutrons from levels in ^{9}Be to the ground state in ^{8}Be: The factor R ranges from 0.6 to 5.9 for the 2.78 MeV level and the 11.81 MeV level, respectively. The effect on the beta decay rate of the broad levels can therefore be considerable.

If levels overlap one must of course resort to the general formalism in order to treat the interference effects correctly. If strong interference is present it becomes questionable to talk about branching ratios to a single level, only the matrix elements have meaning. The case of many levels with many open decay channels is treated by Barker and Warburton [32].

We have already given our prescription for calculating the ft-value, namely by finding B(GT) from the above formulas and extracting ft from eq. (1). This can be shown to correspond to defining an effective f-value of $R\,f_\beta(Q-E_\lambda)$, a method also used in ref. [33]. An alternative definition was used in refs [30,32]; the effective f-value defined there is normalized to the area of the broad level instead of to a narrow level as in our definition (the factor π). With the second definition only the variation of f_β over the level is taken into account, not the one of P_l. Both should be corrected for if one is to compare the resulting ft-values with the ones for narrow levels.

It is important that the levels are identified correctly. For a broad level the decay probability is $w = \frac{\ln 2}{t} = \int w(E)\,dE \propto B(GT)\int f\,dE$, i.e., the B(GT)-value is proportional to $(t\times\int f\,dE)^{-1}$. If the broad level is misinterpreted as consisting of many narrow levels one would construct a beta strength function in stead and get a total B(GT) value of $\int B(GT)\,dE \propto \int (ft)^{-1}\,dE$. The latter expression gives an incorrect result.

The case of the decay of ^{9}Li is more complex than the situation treated up to now. First of all, for each intermediate state several decay channels are open and secondly the levels do not decay into two fragments but three. Most of the levels in ^{8}Be and ^{5}He are actually so broad that it is non-trivial to make a clear distinction between sequential decays through these levels and direct three-body break-up with final-state interactions (in the "sequential picture" the unstable fragment from the first particle emission will only move a few fm before it breaks up itself). See also the discussion in ref. [34]. In want of a full theoretical treatment of the system we have made the approximations to treat each level in ^{9}Be separately and to use the concept of sequential decay. Modifying the simplest one-level multi-channel formula of Lane and Thomas [35], sections XII and XIII.2, to incorporate the beta decay one gets:

$$w(E,E') = \frac{\ln 2}{\pi K} f_\beta(Q-E) \sum_c \frac{G_A^2 B(GT)\, P_c(E-E')\gamma_{\lambda c}^2(E')}{(E_\lambda + \Delta_\lambda(E) - E)^2 + (\frac{1}{2}\Gamma_\lambda(E))^2} \quad , \tag{9}$$

$$\gamma_{\lambda c}^2(E') = \gamma_{\lambda c}^2 \frac{1}{\pi} \frac{P_{\lambda'}(E'-E_{fc})\gamma_{\lambda'}^2}{(E_{\lambda'} + \Delta_{\lambda'}(E') - E')^2 + (\frac{1}{2}\Gamma_{\lambda'}(E'))^2} \quad ,$$

$$\Delta_\lambda(E) = -\sum_c \int dE' (S_c(E-E') - B_c)\gamma_{\lambda c}^2(E') \quad ,$$

$$\Gamma_\lambda(E) = 2\sum_c \int dE' P_c(E-E')\gamma_{\lambda c}^2(E') \quad ,$$

$$\Delta_{\lambda'}(E') = -(S_{\lambda'}(E'-E_{fc}) - B_{\lambda'})\gamma_{\lambda'}^2 \quad , \quad \Gamma_{\lambda'}(E') = 2P_{\lambda'}(E'-E_{fc})\gamma_{\lambda'}^2 \quad .$$

The index c denotes the channel, the index λ' the state in that of the two fragments that subsequently breaks up. The energy E is the excitation energy in the beta-daughter, the energy E' the one in the unstable fragment and the energy E_{fc} the one of the final state after the second break-up in channel c. Otherwise the notation is as before, see also fig. 6b.

To keep the calculations for ^{9}Li tractable only the most important energy dependent factors in equation (9) were kept, namely the penetration-factors in the numerator and the Fermi-factor; the shift factors $\Delta(E)$ were set to zero and the widths $\Gamma(E)$ assumed to be energy-independent. For decay

through ^{5}He, i.e. with beta-decay to a level at E_λ in ^{9}Be and subsequent alpha emission to a level $E_{\lambda'}$ in ^{5}He followed by emission of a neutron, the formula then reduces to:

$$w(E,E') \propto f_\beta(Q-E)\,\frac{P_\alpha(E-E')\Gamma_c}{(E_\lambda-E)^2+\Gamma_\lambda^2/4}\,\frac{P_n(E'-E_f)\Gamma_{\lambda'}}{(E_{\lambda'}-E')^2+\Gamma_{\lambda'}^2/4} \quad . \tag{10}$$

Here Γ_c replaces $\gamma_{\lambda c}^2$ of eq. (9), it parametrizes the relative strength of the channel c. The same formula can be used *mutatis mutandis* for the decays through ^{8}Be.

The measure for the deviation from the narrow level situation corresponding to eq. (8) becomes

$$R'_c = \int_{E_f}^{Q} dE \int_{E_f}^{E} dE'\,\frac{f_\beta(Q-E)}{f_\beta(Q-E_\lambda)}\,\frac{P_\alpha(E-E')}{P_\alpha(E_\lambda-E_{\lambda'})}\,\frac{P_n(E'-E_f)}{P_n(E_{\lambda'}-E_f)}\,\frac{\Gamma_c/2\pi}{(E_\lambda-E)^2+\Gamma_\lambda^2/4}\,\frac{\Gamma_{\lambda'}/2\pi}{(E_{\lambda'}-E')^2+\Gamma_{\lambda'}^2/4} \cdot \tag{11}$$

The branching-ratios for beta decay must be corrected when the B(GT) values are extracted. As the correction factor R'_c will differ for different decay channels, one must know the branching ratios for these different channels in order to find the "effective" correction factor for a state. (This makes it difficult to analyse experiments where only the total decay energy of the states is measured.) The effective correction factor, R', for a state is seen by comparing eqs (9) and (11) to be $R' = \sum_c R'_c$. We do not get the parameters Γ_c from our fit to the data, but can use the particle branching ratios given by $b_c = R'_c/R'$ to find them. As the branching ratios must sum to unity, we need one extra independent equation to determine the Γ's uniquely; this is taken from the requirement $\sum_c \Gamma_c = \Gamma_\lambda$. We should point out that this procedure is only approximate; the reduced transition probability B(GT) can not be determined with good accuracy unless a better theory for three-body decay is used.

Appendix B

Recoil broadening.

Beta-delayed particles from light nuclei can in general be expected to exhibit recoil shifts due to the relatively large recoil-energies of the beta-daughter nuclei. The effect in the decay of ^{9}Li is only visible in the channel through the 2.43 MeV level to the gound state of ^{8}Be; the levels in the remaining decays are too broad. As shown in fig. 5 the recoil effects are appreciable for the mentioned channel. In this appendix the relevant formulas for the calculation of the recoil shifts are given.

The starting point is the intensity, w, as given in ref. [21] for the emission of a delayed particle with kinetic energy shifted by the amount t from the nominal value (units where the speed of light equals one):

$$w \propto F(Z,W)(W_0 - W)^2 pW \frac{1}{2kp_\nu}\left| 1 + A\frac{p}{W}\cos\psi\{-\frac{t}{kp_\nu} - \frac{p}{p_\nu}\cos\psi\}\right| dt dW d\Omega_\beta d\Omega \quad . \tag{12}$$

Here the beta-particle has total energy W (maximum energy W_0), momentum p and angular variables Ω_β, the neutrino has momentum p_ν and the Fermi-function is denoted F(Z,W). The beta-delayed particle has angular variables Ω and ψ is the angle relative to the beta-particle. The variable k is given by

$$k = \sqrt{2\frac{E}{M}\frac{M'(M-M')}{M^2}} \quad ,$$

where M and M' are the masses of the beta-daughter and the emitted particle, respectively, and E is the energy released in the particle decay measured in the centre of mass system. The constant A, which includes the alignment effects, is given by

$$A = \frac{a^2 - (\frac{1}{3} + \frac{2}{30}\tau\theta)c^2}{a^2 + c^2} \quad ,$$

where the nuclear matrix elements are a^2 = B(F) and c^2 = $(G_A/G_V)^2$B(GT) and the coefficients τ and θ are given by Holstein [36]. Neglecting the spin effects one would have $A = -1/3$ for Gamow-Teller decays; for the transition above A is 1/5, i.e. the broadening is enhanced in this case.

The limits on t are $k(\pm(W_0 - W) - p\cos\psi)$. With the angle ψ restricted, by the experimental solid angle, to lie in the interval ψ_{min} to ψ_{max} the intensity for a given energy shift t is given by:

$$\int F(Z,W)\frac{p}{2k}\left|(c_2 - c_1)W(W_0 - W) - A\frac{c_2^{\,2} - c_1^{\,2}}{2}p\frac{t}{k} - A\frac{c_2^{\,3} - c_1^{\,3}}{3}p^2\right| dW \quad . \tag{13}$$

Here

$$c_1 = \min\left\{\cos(\psi_{max}), \max\left|\cos(\psi_{min}), \frac{W - W_0 - t/k}{p}\right|\right\}$$

and

$$c_2 = \max\left\{\cos(\psi_{min}), \min\left|\cos(\psi_{max}), \frac{W_0 - W - t/k}{p}\right|\right\} \quad .$$

The upper limit of the integration in eq. (13) is W_0; the lower limit is m (the electron mass) for $|t/k| \leq W_0 - m$ and

$$\frac{m^2 + (W_0 \pm t/k)^2}{2(W_0 \pm t/k)}$$

otherwise, the plus sign being for t negative and vice versa. The calculated curves in fig. 5 were folded with the resolution function of the experimental set-up.

Figure captions

FIGURE 1

The beta decay scheme of 178.3 ms ^{9}Li including the states fed in the subsequent particle emission. The main information given in this figure is taken from the compilation by Ajzenberg-Selove [15]. The hatched states are broad (the widths are given in table 1).

FIGURE 2

Energy spectrum of beta-delayed neutrons from ^{9}Li measured with a ^{3}He spectrometer. The spectrum has been corrected for the detector efficiency and the thermal peak has been subtracted. The full drawn curve shows the fit to the spectrum when all contributions from intermediate states in ^{9}Be, ^{8}Be and ^{5}He have been taken into account.

FIGURE 3

Electron scattering spectrum from ^{9}Be(e,e') obtained by summing three spectra measured at the incident energies and scattering angles E_0,θ = 45 MeV, 105°; 45 MeV, 129° and 49 MeV, 117°, respectively, in order to obtain a summed spectrum of good statistical accuracy. Due to the proximity of the 1.68 MeV, $J^{\pi} = 1/2^{+}$ level near the threshold for the decay into ^{8}Be + n the line shape of the level is strongly asymmetric (for details see ref. [19]).

FIGURE 4

Energy spectrum of beta-delayed alpha particles from ^{9}Li. The spectrum was measured with a surface-barrier detector telescope operated in anticoincidence mode to avoid summing with beta particles. The alphas originate partly from direct delayed alpha emission in the decay channel ^{5}He + α, and partly from the break-up of the delayed particle daughters ^{8}Be and ^{5}He into $\alpha + \alpha$ and α + n, respectively. The inset shows the high energy part together with a fit taking the 11.28 MeV and 11.81 MeV states into account.

FIGURE 5

The low energy part of the beta-delayed neutron spectrum. The inset shows the energy region around the 682 keV peak corresponding to the $^{9}Be(5/2^{-}) \rightarrow {}^{8}Be(g.s.)$ transition. Due to the short life-time of the 2.43 MeV ($5/2^{-}$) state the peak is broadened by recoil and polarization effects. The background-corrected experimental spectrum is denoted by squares and the fit, including detector resolution, recoil and alignment effects, is givn by the solid line. The expected peak shape from detector resolution alone (in this measurement FWHM = 30 keV) is given by the narrow peak.

FIGURE 6

Illustration of a) beta-delayed single particle emission and b) beta-delayed two particle emission (sequential emission only). The strong lines indicate the particle emission, the levels are denoted as in the text.

Table captions

TABLE 1

Excitation energies and widths of intermediate states populated in the beta-delayed particle-emission of ^{9}Li.

TABLE 2

Experimentally determined branching ratios for the beta decay of ^{9}Li to states in ^{9}Be. The $B(GT)-$ and $\log ft-$values are deduced taking the variation of the statistical rate function over the width of the states into account.

References

1. P.G.Hansen and B.Jonson, Vol.III p.157 in "Particle Emission from Nuclei", eds. M.Ivascu and D.Poenaru (CRC Press, 1988).
2. I.Tanihata, H.Hamagaki, O.Hashimoto, Y.Shida, N.Yoshikawa, K.Sugimoto, O.Yamakawa, T.Kobayashi and N.Takahashi, Phys.Rev.Lett **55** (1985) 2676.
3. P.G.Hansen and B.Jonson, Europhys. Lett. **4** (1987) 409.
4. W.L.Gardner, N.Knable and B.J.Moyer, Phys.Rev. **83** (1951) 1054.
5. R.Middleton and D.J.Pullen, Nucl.Phys. **51** (1964) 50.
6. A.H.Wapstra and G.Audi, Nucl.Phys. **A432** (1985) 1.
7. D.E.Alburger, Phys.Rev. **132** (1963) 328.
8. D.E.Alburger and D.H.Wilkinson, Phys.Rev **C13** (1976) 835.
9. Y.S.Chen, T.A.Tombrello and R.W.Kavanagh, Nucl.Phys. **A146** (1970) 136.
10. B.E.F.Macefield, B.Wakefield and D.H.Wilkinson, Nucl.Phys. **A131** (1969) 250.
11. T.Bjørnstad, H.Å.Gustafsson, P.G.Hansen, B.Jonson, V.Lindfors, S.Mattsson, A.M.Poskanzer and H.L.Ravn, Nucl.Phys. **A359** (1981) 1.
12. M.Langevin, C.Détraz, D.Guillemaud, F.Naulin, M.Epherre, R.Klapisch, S.K.T.Mark, M.de Saint Simon, C.Thibault and F.Touchard, Nucl.Phys. **A366** (1981) 449.
13. D.Mikolas, B.A.Brown, W.Benenson, L.H.Harwood, E.Kashy, J.A.Nolen Jr., B.Sherill, J.Stevenson, J.S.Winfield, Z.Q.Xie and R.Sherr, Phys.Rev. **C37** (1988) 766.
14. H.L.Ravn, Phys.Rep. **54** (1979) 203.
15. F.Ajzenberg-Selove, Nucl.Phys. **A490** (1988) 1.
16. H.Franz, W.Rudolph, H.Ohm, K.-L.Kratz, G.Herrmann, F.M.Nuh, D.R.Slaughter and S.G.Prussin, Nucl.Instr.Methods **144** (1977) 253.
17. K.-H.Beimer, G.Nyman and O.Tengblad, Nucl.Instr.Methods **A245** (1986) 402.
18. O.Tengblad, K.-H.Beimer and G.Nyman, Nucl.Instr.Methods **A258** (1987) 230.
19. G.Kuechler, A.Richter and W. von Witsch, Z.Phys. A - Atomic Nuclei **326** (1987) 447.

20. G.Nyman, R.E.Azuma, B.Jonson, K.-L.Kratz, P.O.Larsson, S.Mattsson and W.Ziegert, Proc. 4th Int. Conf. on Nuclei Far from Stability, (Ed. P.G.Hansen and O.B.Nielsen) CERN 81 – 09 (1981) p.312.

21. E.T.H.Clifford, J.C.Hardy, H.Schmeing, R.E.Azuma, H.C.Evans, T.Faestermann, E.Hagberg, K.P.Jackson, V.T.Koslowsky, U.J.Schrewe, K.S.Sharma and I.S.Towner, Phys.Rev.Lett. **50** (1983) 23;

E.T.H.Clifford, thesis, University of Toronto (1981) unpublished;

E.T.H.Clifford, E.Hagberg, J.C.Hardy, H.Schmeing, R.E.Azuma, H.C.Evans, V.T.Koslowsky, U.J.Schrewe, K.S.Sharma and I.S.Towner, Nucl.Phys **A493** (1989) 293.

22. O.V.Bochkarev, A.A.Korshennnikov, E.A.Kuz'min, I.G.Mukha, A.A.Ogloblin, L.V.Chulkov and G.B.Yan'kov, Yad.Fiz. **46** (1987) 12 [English translation, Sov.J.Nucl.Phys. **46** (1987) 7].

23. D.H.Wilkinson and B.E.F.Macefield, Nucl.Phys. **A232** (1974) 58.

24. D.H.Wilkinson, Phys.Lett. **31B** (1970) 447.

25. D.H.Wilkinson, Phys.Rev.Lett. **27** (1971) 1018.

26. I.S.Towner, Nucl.Phys. **A216** (1973) 589.

27. K.Riisager, J.Phys. **G14** (1988) 1301.

28. A.Sirlin, Phys.Rev. **D35** (1987) 3423.

29. P.Bopp, D.Dubbers, L.Hornig, E.Klemt, J.Last, H.Schütze, S.J.Freedman and O.Schärpf, Phys.Rev.Lett. **56** (1986) 919.

30. F.C.Barker, Aust.J.Phys. **22** (1969) 293.

31. F.C.Barker, Aust.J.Phys. **24** (1971) 777.

32. F.C.Barker and E.K.Warburton, Nucl.Phys. **A487** (1988) 269.

33. E.K.Warburton, Phys.Rev. **C33** (1986) 303.

34. D.Robson, in Nuclear Spectroscopy and Reactions, ed. J.Cerney, part D (Academic Press New York,1975) p.179.

35. A.M.Lane and R.G.Thomas, Rev.Mod.Phys. **30** (1958) 257.

36. B.R.Holstein, Rev.Mod.Phys. **46** (1974) 789.

Isotope	E_{ex} (MeV±keV)	Γ (keV)
^{9}Be	2.43±15 2.78±120 7.94±80 11.28±24 11.81±20	0.77±0.15 1080±110 ~1000 575±50 400±30
^{8}Be	ground state 2.94±30	$(6.8\pm1.7)*10^{-3}$ 1560±30
^{5}He	ground state 4±1	600±20 4000±1000

Table 1

E^* (MeV)	I^π	Γ_{cm} (keV)	I_β [c] (%)	B(GT) corrected	log*ft*
0.0	$3/2^-$	-	50±3	0.019±0.002	5.32
1.68	$1/2^+$	217±0.10	‹ 2		
2.43	$5/2^-$	0.77±0.15	30±3	0.029±0.003	5.13
2.78	$1/2^-$	1080±110	16±3	0.007±0.003	5.8
7.94	$(1/2^-)$[a]	~1000	‹ 2	‹ 0.25	
11.28	$(3/2^-)$[a]	575±50	1.1±0.2	0.9±0.3	3.6
11.81	[b]	400±30	2.7±0.2	5.6±1.2	2.84

[a] Langevin et al. Ref. 12
[b] Not known
[c] The quoted errors do not include uncertainties due to limitations of the applied model

Table 2

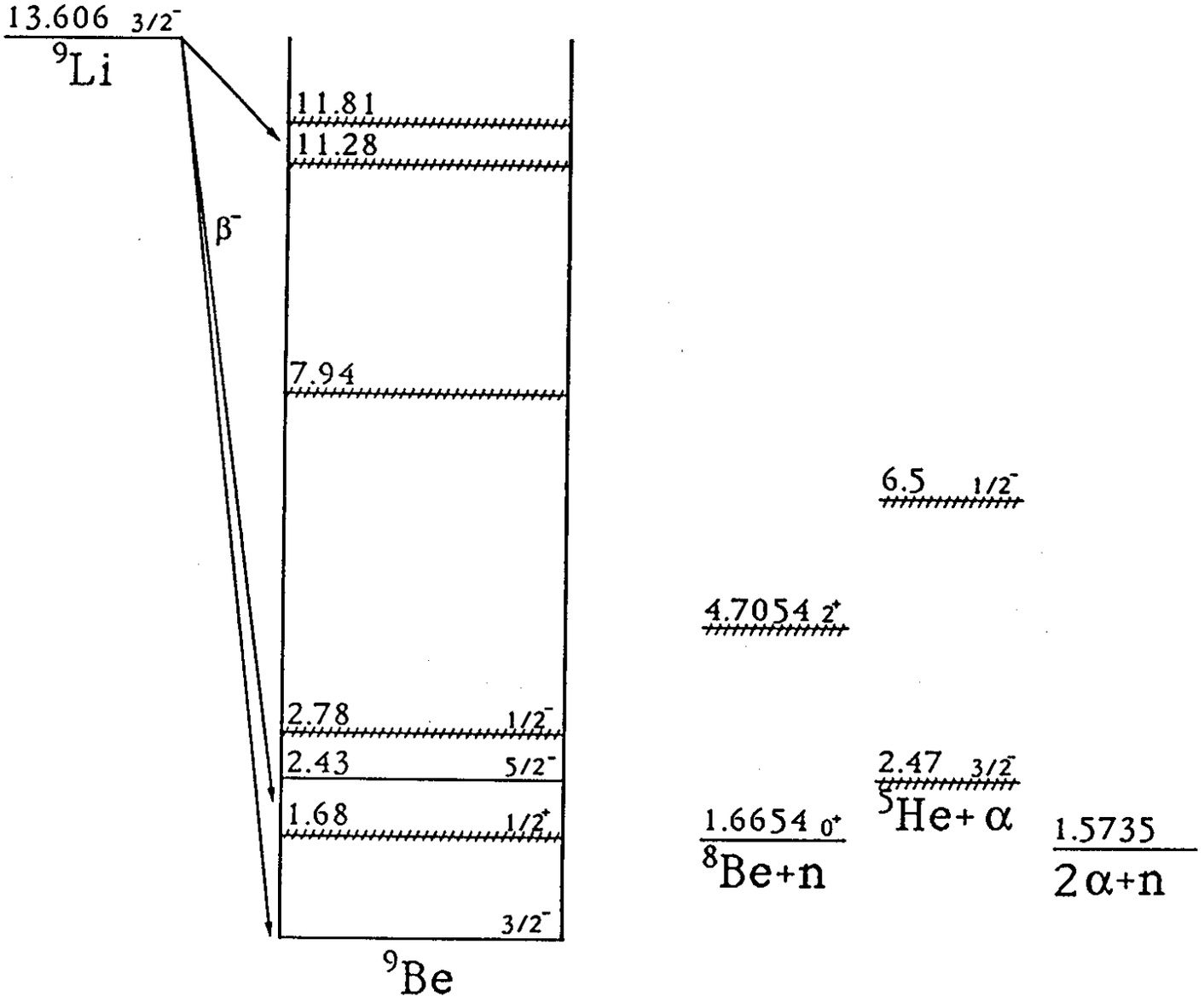
13.606 3/2⁻
⁹Li
β⁻
11.81
11.28
7.94
2.78 1/2⁻
2.43 5/2⁻
1.68 1/2⁺
3/2⁻
⁹Be
6.5 1/2⁻
4.7054 2⁺
2.47 3/2⁻
1.6654 0⁺
⁸Be+n
⁵He+α
1.5735
2α+n

Figure 1

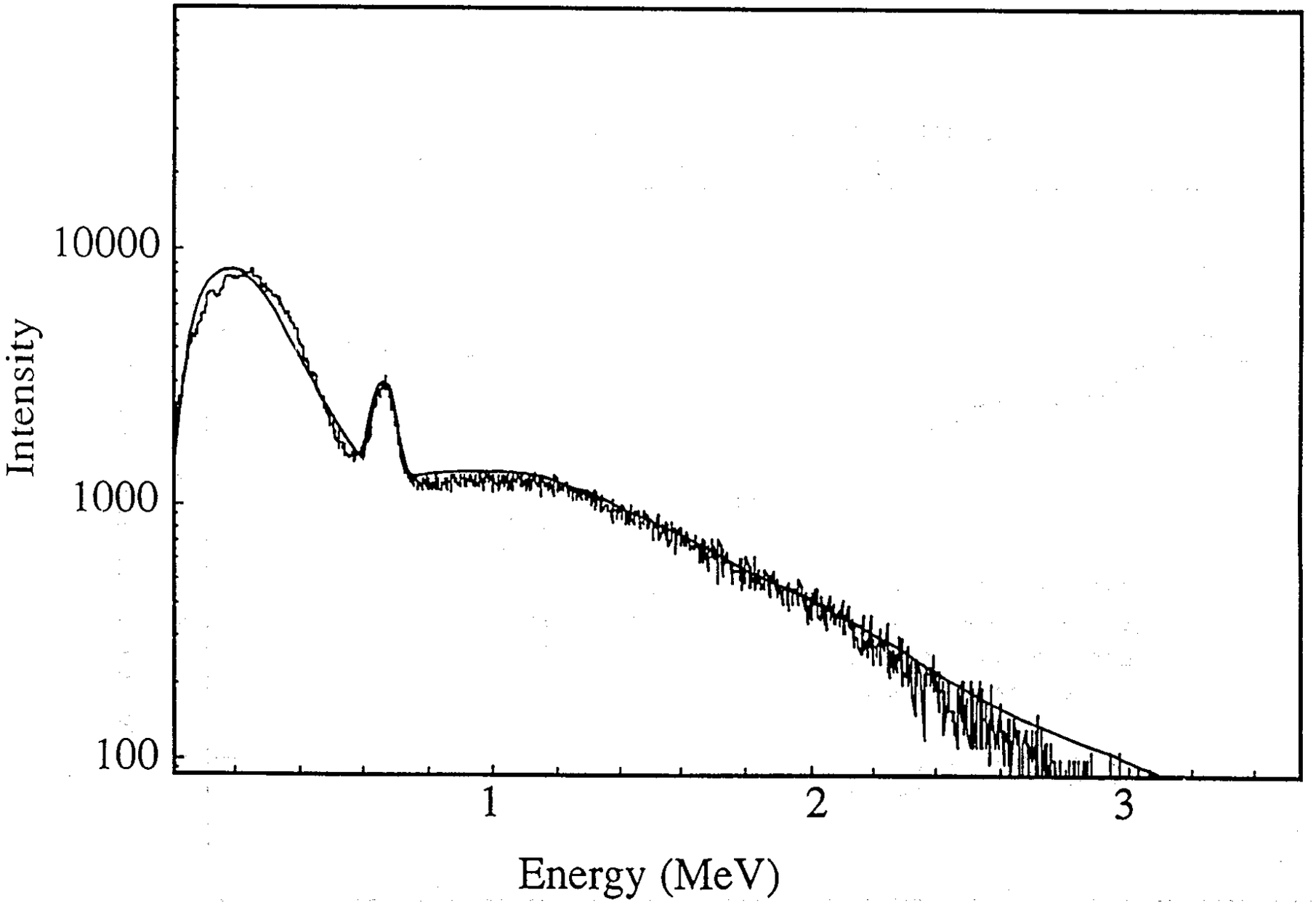

Figure 2

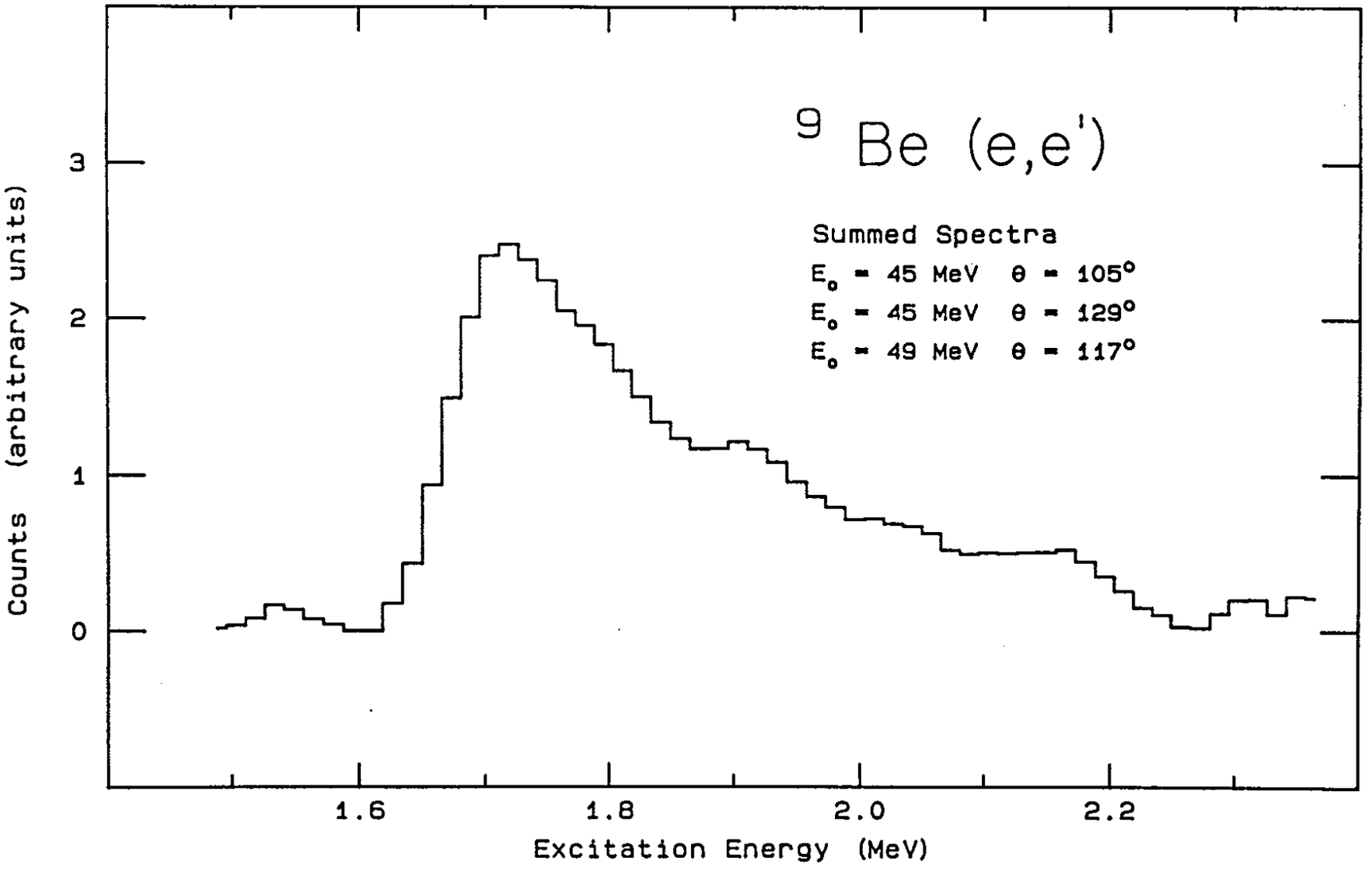
^{9} Be (e,e')
Summed Spectra
E_o = 45 MeV θ = 105°
E_o = 45 MeV θ = 129°
E_o = 49 MeV θ = 117°
Counts (arbitrary units)
0
1
2
3
1.6
1.8
2.0
2.2
Excitation Energy (MeV)

Figure 3

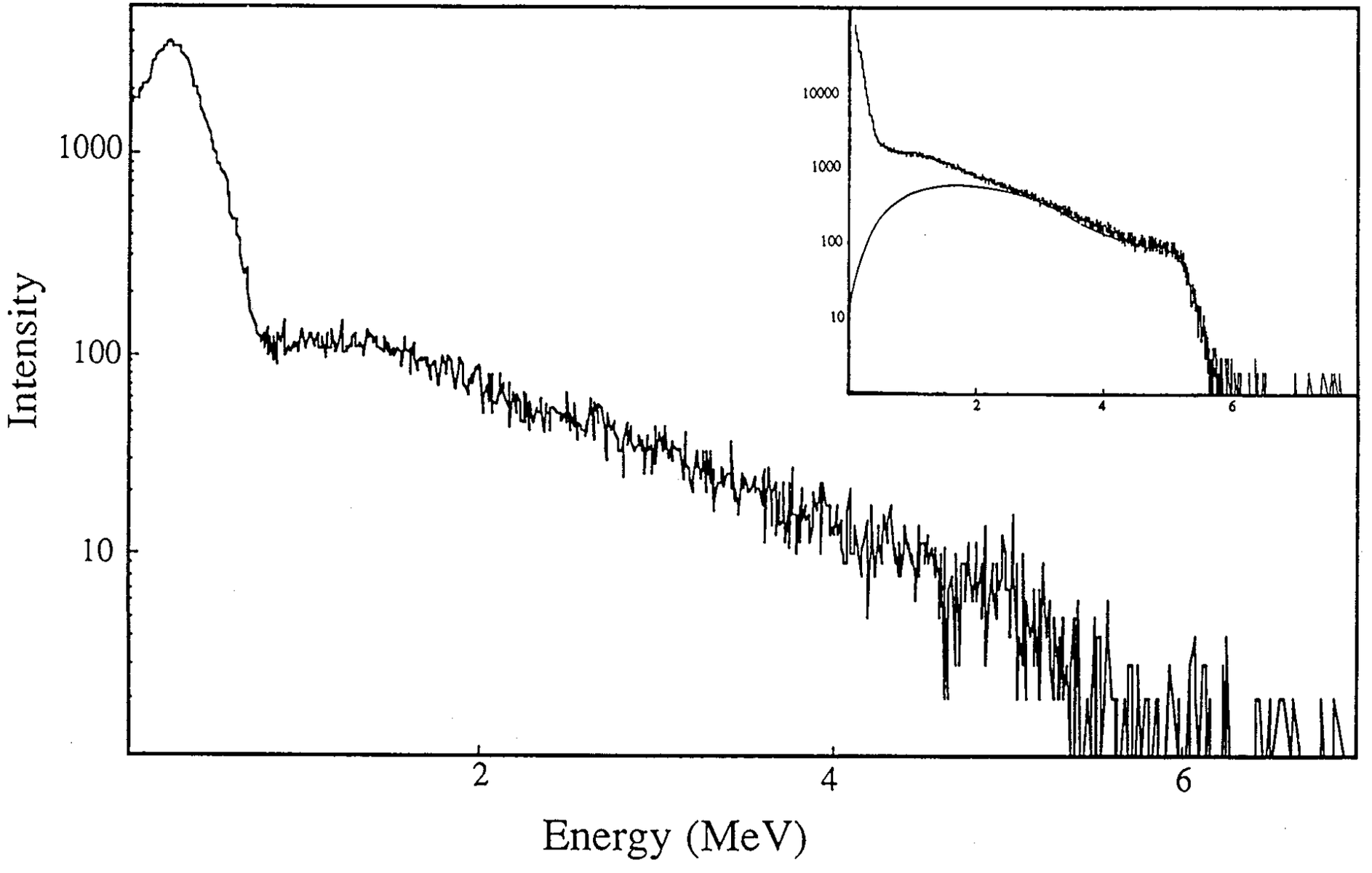

Figure 4

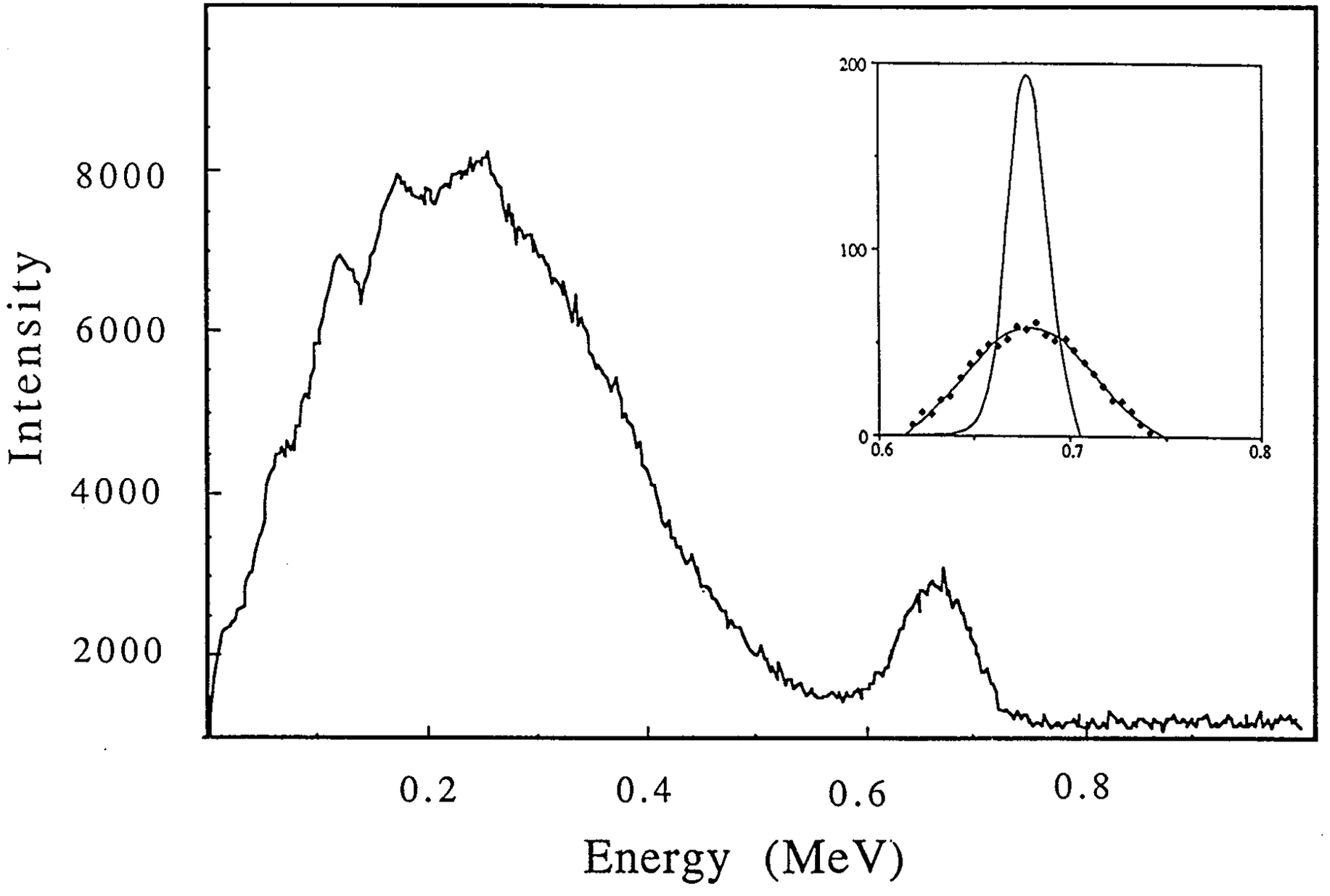
Intensity
8000
6000
4000
2000
0.2
0.4
0.6
0.8
Energy (MeV)
200
100
0
0.6
0.7
0.8

Figure 5

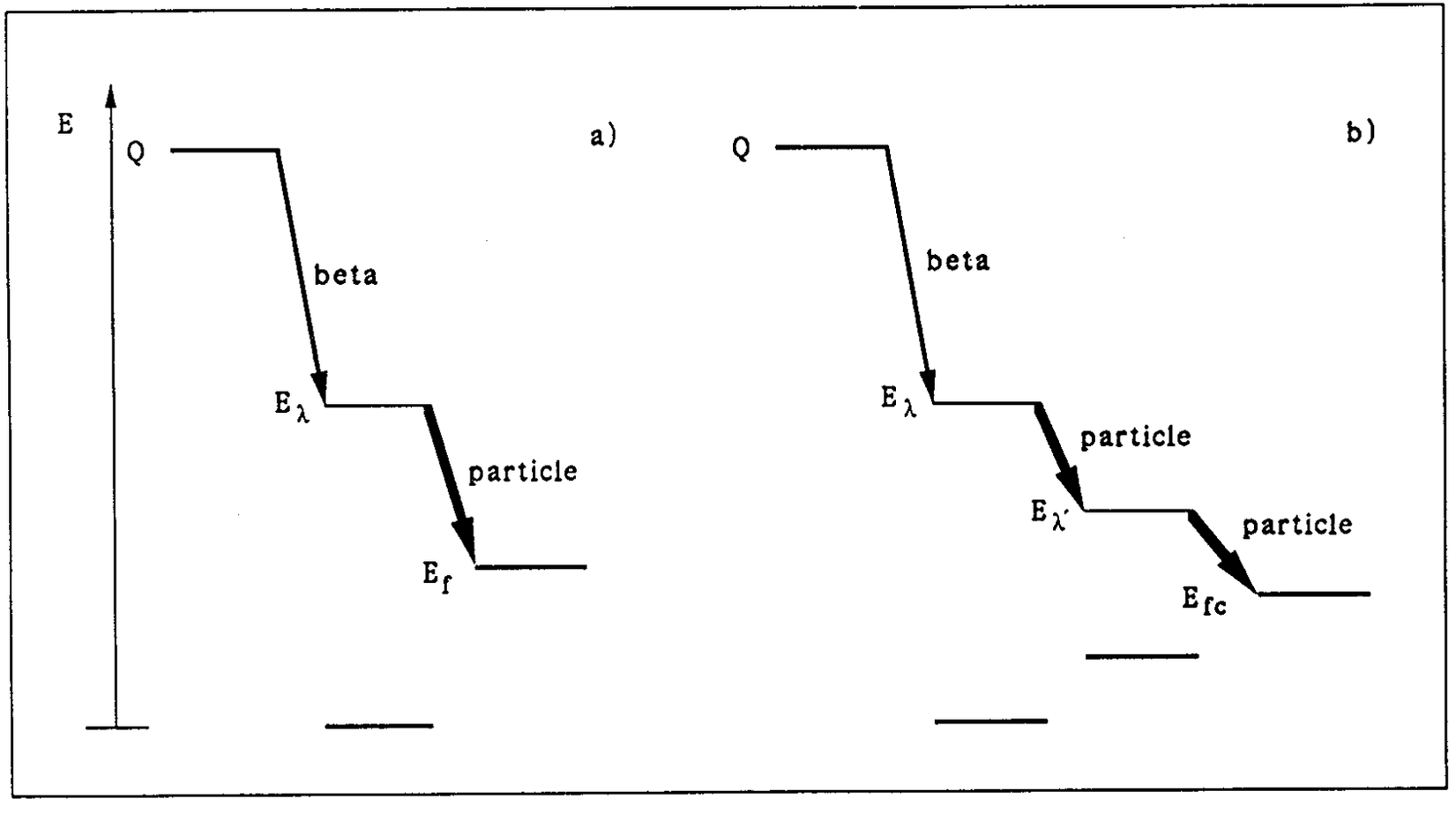
E
Q
a)
beta
E_λ
particle
E_f
Q
b)
beta
E_λ
particle
$E_{\lambda'}$
particle
E_{fc}

Figure 6